

## Micro-Turbine Generation using Simulink

S.A. Shakur<sup>1</sup> and Dr. Sanjay K. Jain<sup>2</sup>

*Electrical and Instrumentation Dept.,  
Thapar University, Patiala, Punjab, India  
E-mail: <sup>1</sup>syedabdulshakur@gmail.com, <sup>2</sup>skjain@thapar.edu*

### Abstract

Microturbine technology is becoming more potential and viable distributed energy source in the recent years. This is due to their salient features such as high operating efficiency, ultra low emission levels, low initial cost and small size. Micro-turbines are small high-speed versions of conventional heavy-duty gas turbines. Hence the dynamic model of a conventional gas turbine, with relatively small thermodynamic constants, can be adopted to study the impacts of a microturbine on the overall system. A model of a heavy-duty gas turbine suitable is presented for use in dynamic power studies.

**Keywords:** Microturbine, Gas turbine, Distributed Generation, Renewable Generation.

### Introduction

The small gas-fired micro-turbines ranging in size from 25-500 kW will provide the electric power industry with a variety of opportunities to meet the challenges of the competitive market. These generators have a low initial cost and are highly efficient, multi-fuelled, reliable and light weight. It takes very clever engineering and use of innovative design (e.g. air bearing, recuperation) to achieve reasonable efficiency and costs in machines of lower output. A big advantage of these systems is small-sized because these technologies mainly use high-speed turbines (50,000-120,000 RPM) with air foil bearings. Therefore, micro-turbines are one of the most promising of the renewable electric generation technologies for applications today [1]. Fig. 1 shows a block diagram of micro-turbine system that consists of air compressor, recuperator, combustor, turbine, generator, and a PCU (Power Conditioning Unit) and its features are summarized below.

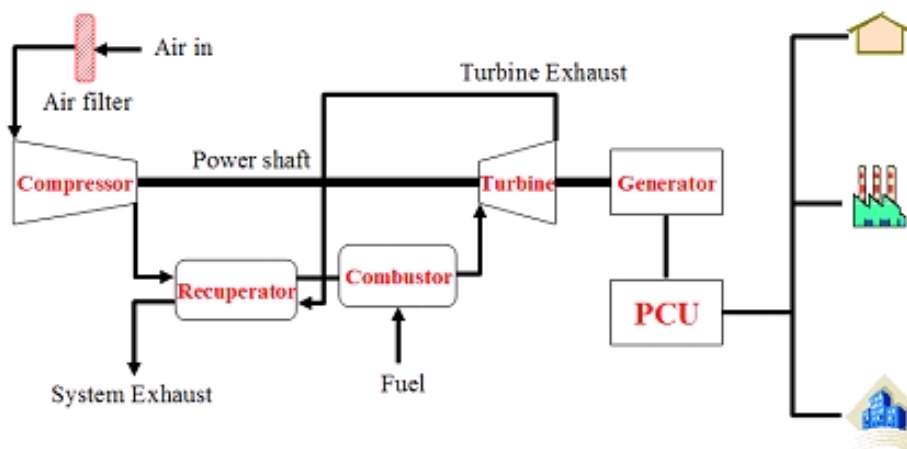


**Figure 1:** Block diagram of micro-turbine system

Microturbine is a typical and practical solution because of its environment-friendliness and high energy efficiency [1], [2]. Various applications such as peak saving, co-generation, remote power and premium power will make its use worldwide. An accurate model of the micro turbine is therefore required to analyze the mentioned impacts. A dynamic model for combustion gas turbine has been discussed in [3]-[6]. In these references, a combustion gas turbine model was used to represent the gas turbine dynamics, including speed, temperature, acceleration and fuel controls. However these works deal with heavy-duty gas turbine. Modeling of micro turbine was reported in [8], [10] where the author developed a generic model of the grid connected micro turbine converter.

The electric generator used in a modern MTG system is usually a permanent magnet synchronous machine (PMSM). The detailed equations to model a PMSM have been summarized in [7], [9]. Synchronism of converter control with the grid is achieved by using a PLL [11].

### **Construction and Principle of micro turbine unit**

The basic components of a micro turbine are the compressor, combustor, turbine generator and recuperate as shown in Fig. 2. It operates on the same principles as traditional gas turbines [2]. Air is drawn into compressor; where it is pressurized and forced into the cold side of recuperate. Here exhaust heat is used to preheat the air before it enters the combustion chamber. The combustion chamber then mixes the heated air with fuel and burns it. This mixture expands through the turbine, which drives the compressor and generator [3].

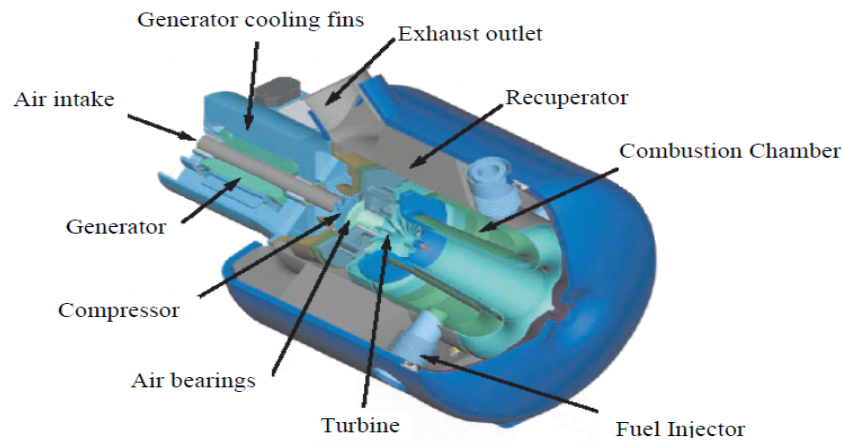


**Figure 2:** Components of Micro Turbine

**Modeling of MTG System**

The integrated MTG system consists of Microturbine, Permanent magnet synchronous machine, Machine and Grid side converters Control and Filter as shown in Fig. 3.

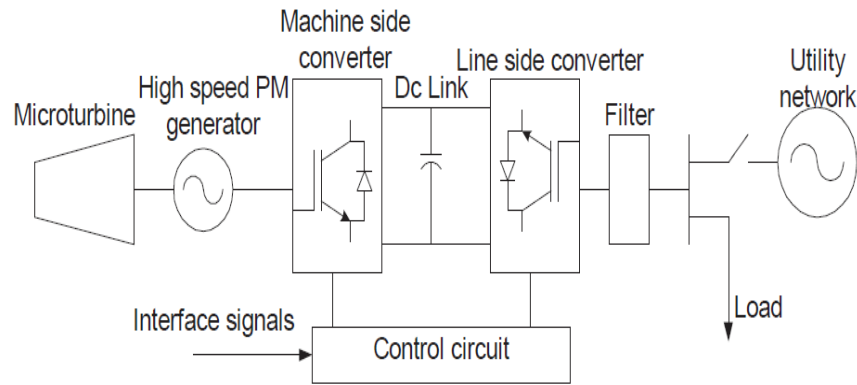


**Figure 3:** Integrated MTG system

**Control functions of the Microturbine**

The control functions of the microturbine are: speed control acting under part load conditions, temperature control acting as an upper output power limit, and acceleration control to prevent over speeding. The output of these control function blocks are all inputs to a least value gate (LVG), whose output is the lowest of the three inputs and results in the least amount of fuel to the compressor-turbine as shown in Fig. 4. This figure shows the per-unit representation of a microturbine, along with its control systems [5].

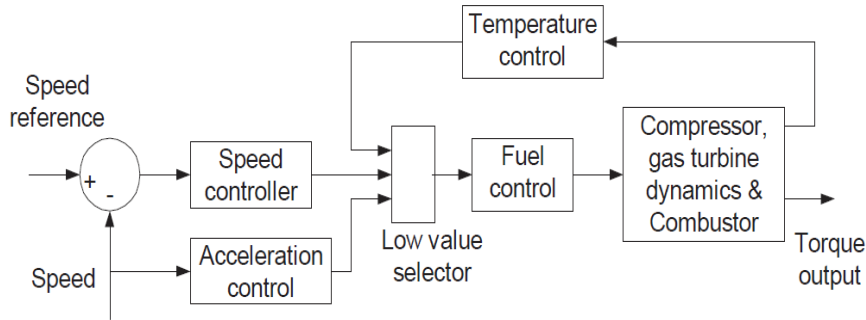


**Figure 4:** Control functions of microturbine

The speed control operates on the speed error formed between a reference (one per-unit) speed and the MTG system rotor speed. It is the primary means of control for the microturbine under part load conditions. Speed control is usually modelled by using a lead-lag transfer function or by a PID controller. In this work a lead lag transfer function has been used to represent the speed controller, as shown in Fig. 5. In this figure  $K$  is the controller gain,  $T_1$  ( $T_2$ ) is the governor lead (lag) time constant, and  $Z$  is a constant representing the governor mode (droop or isochronous) [5].

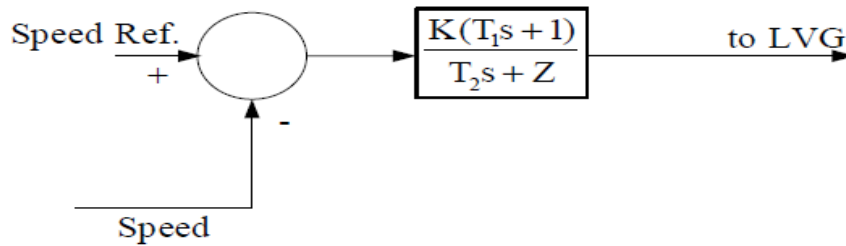


**Figure 5:** Speed controller for the microturbine

The fuel system consists of the fuel valve and actuator as shown in Fig. 6. The fuel flow out from the fuel system results from the inertia of the fuel system actuator and of the valve positioner, whose equations are given below.

The valve positioner transfer function is:

$$E_1 = \frac{K_v}{T_v s + c} F_d$$

And the fuel system actuator transfer function is:

$$Wf = \frac{K_f}{T_f s + c} E_1$$

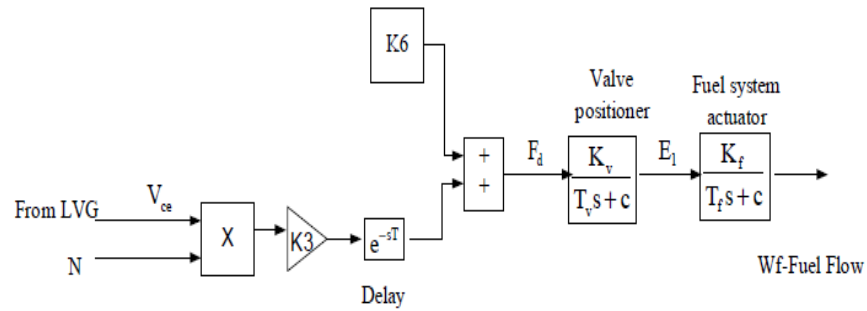


**Figure 6:** Block diagram of the Fuel system

The compressor-turbine is the heart of the microturbine and is essentially a linear, nondynamic device (with the exception of the rotor time constant). There is a small transport delay TCR, associated with the combustion reaction time, a time lag TCD, associated with the compressor discharge volume and a transport delay TTD , for transport of gas from the combustion system through the turbine [6]. The block diagram of the compressor-turbine package is shown in Fig. 7.

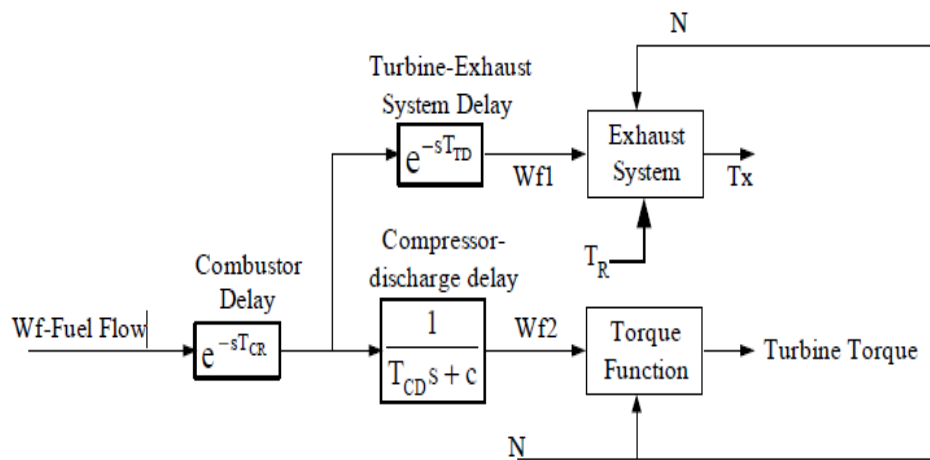


**Figure 7:** Compressor-Turbine package of a microturbine

Temperature control is the normal means of limiting the gas turbine output power at a predetermined firing temperature, independent of variation in ambient temperature or fuel characteristics. The fuel burned in the combustor results in turbine torque and in exhaust gas temperature. The exhaust temperature is measured using a series of thermocouples incorporating radiation shields as shown in the block diagram of the temperature controller [6].

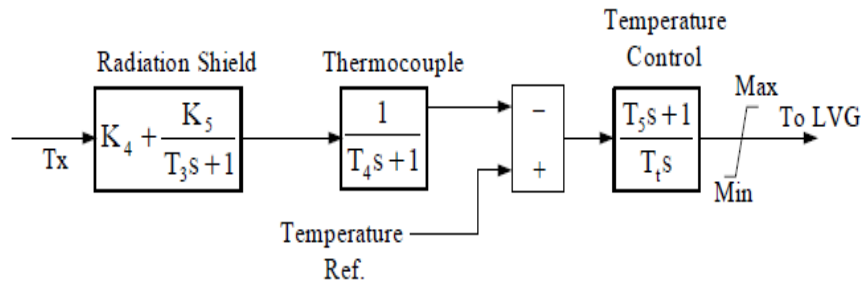


**Figure 8:** Block diagram of the temperature controller

The implementation of microturbine model using Simulink of the Matlab is shown in Fig 9.

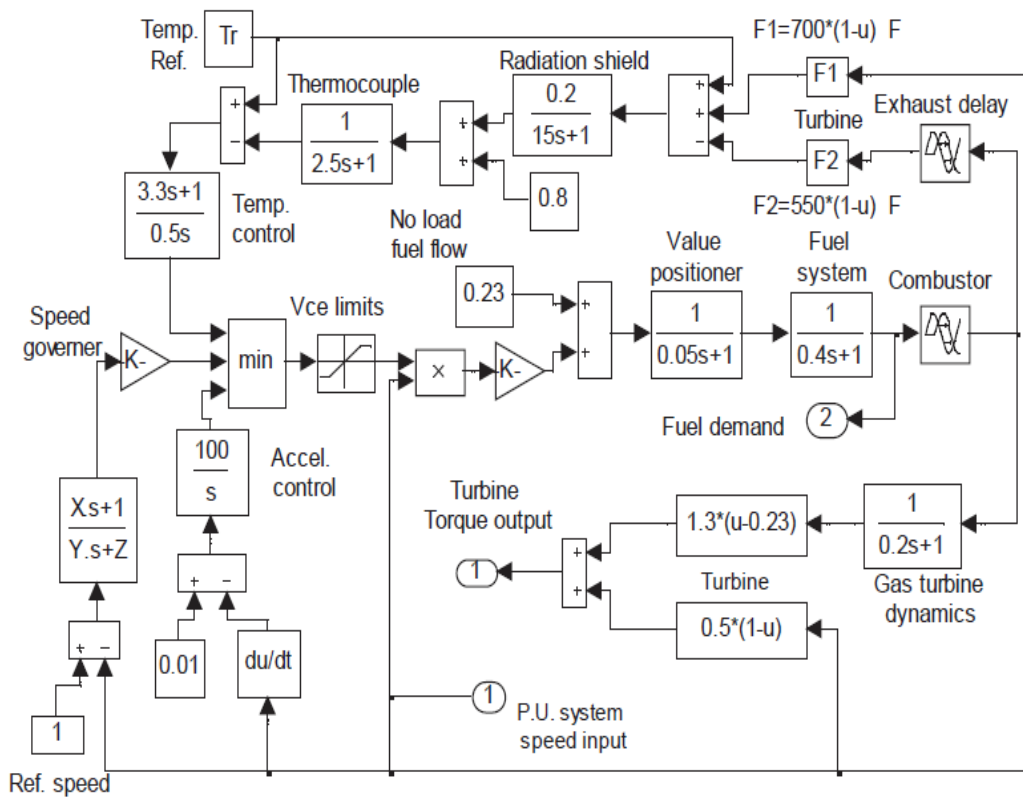


**Figure 9:** Simulink model of the microturbine

**Permanent Magnet Synchronous Machine (PMSM)**

Microturbine produces electrical power via a high-speed generator directly driven by the turbo-compressor shaft. Small gas turbines benefit in particular when the gearbox

that reduces the shaft speed to the speed of conventional electrical machines is eliminated, as is the case with the single-shaft designs considered here. In a permanent magnet synchronous machine, the dc field winding of the rotor is replaced by a permanent magnet. The advantages are elimination of field copper loss, higher power density, lower rotor inertia, and more robust construction of the rotor. The drawbacks are loss of flexibility of field flux control and possible demagnetization. The machine has higher efficiency than an induction machine, but generally its cost is higher [7].

**dq Axis Representation of a PMSM.** In a PMSM, the permanent magnets are glued on the rotor in surface sinusoidal magnet machine (SPM), and are mounted inside the rotor in case of an interior or buried magnet synchronous machine (IPM). The stator has three phase sinusoidal winding, which creates a synchronously rotating air gap flux. If the machine is rotated by a prime mover, the stator windings generate balanced three-phase sinusoidal voltages. The dq axis representation of a permanent magnet synchronous machine (for a balanced system the 0-axis quantities are equal to zero) [9].

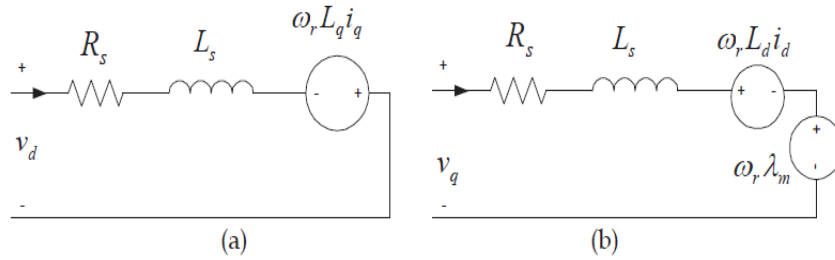


**Figure 10:** dq-axis equivalent circuit model of the PMSM a) d-axis b) q-axis

$$V_d = R_s i_d + L_d \frac{di_d}{dt} - p \omega_r L_q i_q$$

$$V_q = R_s i_q + L_d \frac{di_q}{dt} + p \omega_r L_d i_d + p \omega_r \phi_m$$

Where, the stator resistance is denoted by  $R_s$ , the  $d$ -axis and  $q$ -axis inductances are  $L_d$  and  $L_q$  respectively,  $\phi_m$  is the flux linkage due to the permanent magnets,  $v_d$  and  $v_q$  are  $dq$  axis voltages. In the  $dq$ -frame, the expression for electro-dynamic torque becomes:

$$T_e = 1.5 p (\phi_m i_q + (L_d - L_q) i_d i_q)$$

The equation for motor dynamics can be given as:

$$\frac{d}{dt} \omega_r = \frac{1}{J} (T_e - F \omega_r - T_M)$$

$$\frac{d}{dt}\theta_r = \omega_r$$

$$\begin{bmatrix} v_q \\ v_d \\ v_o \end{bmatrix} = \frac{2}{3} \begin{bmatrix} \cos\theta_r & \cos(\theta_r - 120) & \cos(\theta_r + 120) \\ \sin\theta_r & \sin(\theta_r - 120) & \sin(\theta_r + 120) \\ 1/2 & 1/2 & 1/2 \end{bmatrix} \begin{bmatrix} v_a \\ v_b \\ v_c \end{bmatrix}$$

$$\begin{bmatrix} v_a \\ v_b \\ v_c \end{bmatrix} = \begin{bmatrix} \cos\theta_r & \sin\theta_r & 1 \\ \cos(\theta_r - 120) & \sin(\theta_r - 120) & 1 \\ \cos(\theta_r + 120) & \sin(\theta_r + 120) & 1 \end{bmatrix} \begin{bmatrix} v_q \\ v_d \\ v_o \end{bmatrix}$$

Where  $p$  is the number of pole pairs,  $Te$  is the electromagnetic torque,  $F$  is combined viscous friction of rotor and load,  $\omega r$  is the rotor speed, and  $J$  is the moment of inertia,  $\theta r$  is rotor angular position and  $Tm$  is shaft mechanical torque. The  $d, q$  variables are obtained from  $a, b, c$  variables through the Park transform and  $a, b, c$  variables are obtained from the  $d, q$  variables through the inverse of the Park transform [7], [9].

### Machine Side Converter Control

Fig. 11 shows the Machine side converter controller implemented in Simulink of the Matlab.

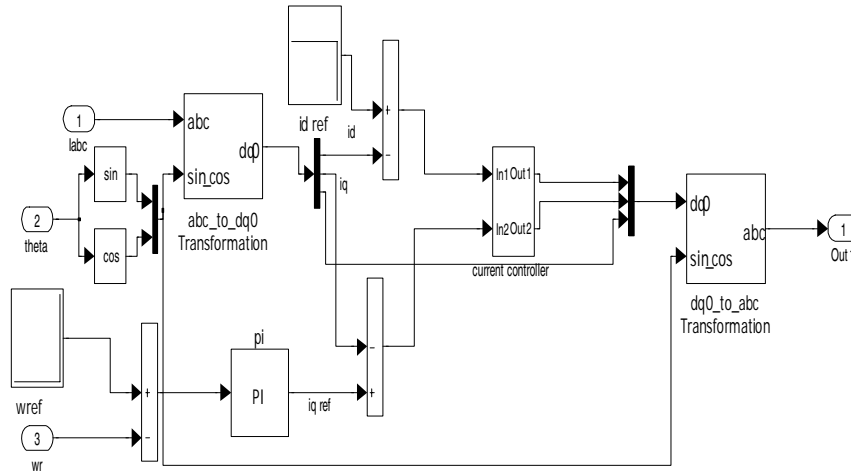


**Figure 11:** Machine side converter controller implemented in simulink

In this system the following PI controller is employed as the speed controller.

$$i_{qref} = K_{p\omega} e_{\omega} + K_{i\omega} \int e_{\omega} dt$$

Where  $K_{p\omega}$  and  $K_{i\omega}$  are the proportional and integral gains of the speed controller respectively while  $e_\omega$  is the error between the reference speed and measured speed. The commanded optimal d-axis current  $i_{dref}$  is obtained from the maximum allowed phase voltage and phase current constraints of the drive.

$$i_d = -\frac{\lambda_m}{L_d} + \sqrt{\left(\frac{V_{max}}{\omega L_d}\right)^2 - \left(\frac{L_q}{L_d} i_q\right)^2}$$

$$v_d = K_{pi} e_{id} + K_{li} \int e_{id} dt - \omega_r L_q i_q$$

$$v_q = K_{pi} e_{iq} + K_{li} \int e_{iq} dt + \omega_r (L_d i_d + \lambda_m)$$

Where  $K_{pi}$  and  $K_{li}$  are the proportional and integral gains of the controller respectively.  $e_{id} = i_{dref} - i_d$  is the d-axis current error and  $e_{iq} = i_{qref} - i_q$  is the q-axis current error.

### Line Side Converter Control

The objective of the supply-side converter is to keep the DC-link voltage constant, regardless of the magnitude and direction of the rotor power. A vector control approach is used here, with the reference frame oriented along the stator voltage vector position [8].

**Grid connected mode:** The PQ control strategy with DC link voltage control is employed for grid connected operation of MTG system. In this scheme the power injected to the grid is regulated by controlling the injected current. The control structure for grid-connected mode operation of MTG system is shown in Fig. 12.

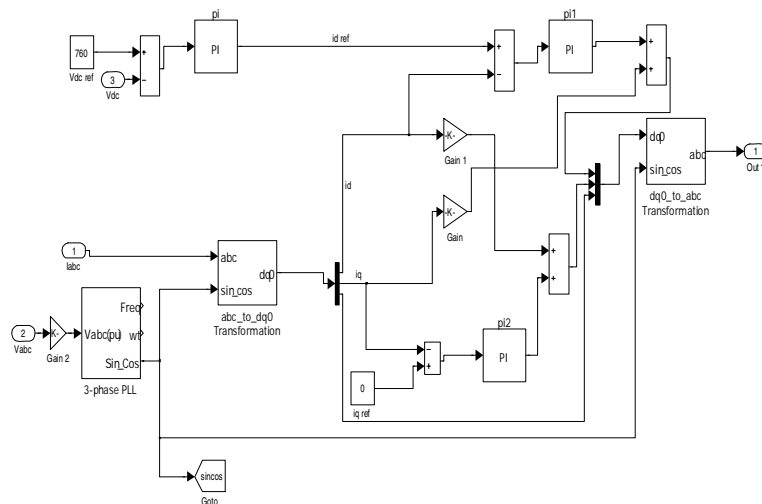


Figure 12: Control Structure for Grid mode operation



One of the important requirements in the interconnection design of the power electronic converter interfaced renewable electric generation system is that of synchronization to the utility system. Synchronism of converter control with the grid is achieved by using a PLL. The Simulink block diagram of the PLL used in this work is shown in Fig. 14, where  $\gamma$  is the grid phase angle,  $V_x$  and  $V_y$  are the grid voltage components in the stationary reference frame [11].

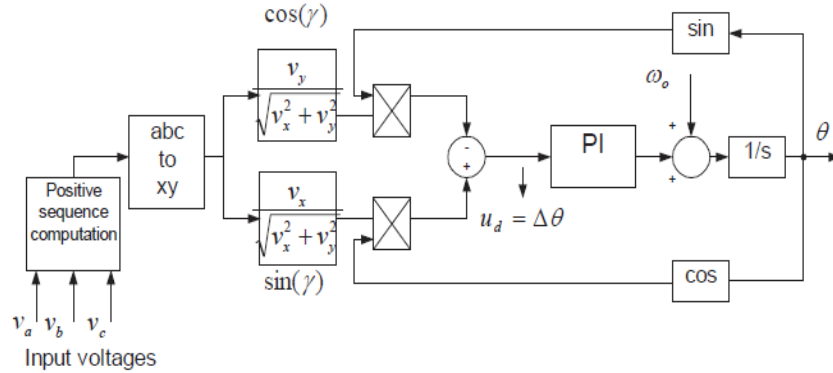


Figure 14: PLL implemented in simulink

### Simulation of MTG

Fig. 15 shows the simulation model implemented in the SimPowerSystems of the MATLAB to study the performance of the MTG system operation in grid connected mode. The utility network, to which the MTG system is connected, is represented by a 3 phase sinusoidal source with its impedance. The series RL filter is used at the grid side of the MTG system. The simulation parameters of the model are given in Appendix.

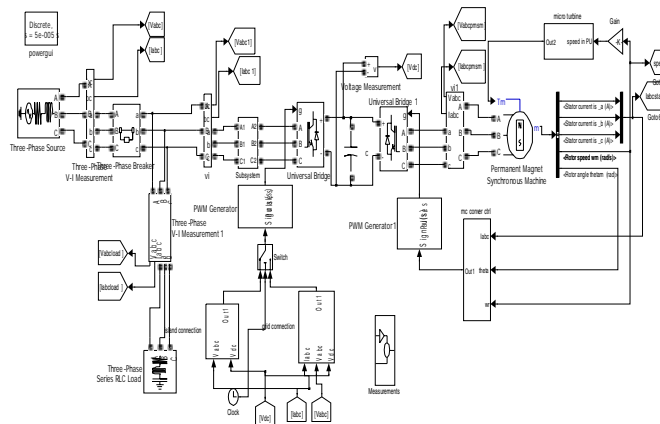
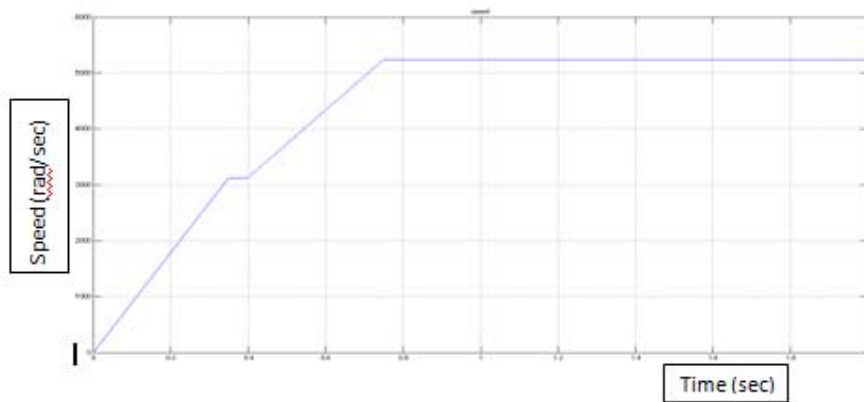


Figure 15: Matlab/SimPowerSystems implementation of MTG system connected to grid

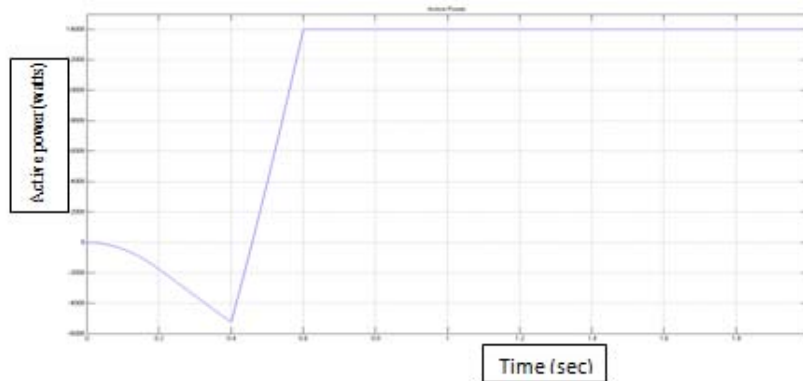
## Results and Discussions

The model used for the performance of MTG system is shown in Fig. 15. The MTG system is connected to 3- $\phi$  utility having voltage as 480 volt and local load of 10 kW. The Speed (rad/sec) – Time characteristics of microturbine is shown in Fig. 16.

The Fig. 16 shows the microturbine reaches the set value of speed of 3100 in 0.35 sec Till 0.4 sec. MTG absorbs 5.2 kW power from grid as shown in Fig. 17. This suggests that microturbine system is operating in motoring mode. When PMSM is switched to Generating mode as shown in fig. 16, the power flows from MTG system to Grid. In generating mode MTG Generates 14 kW of power to the Grid as shown in fig. 3.17.

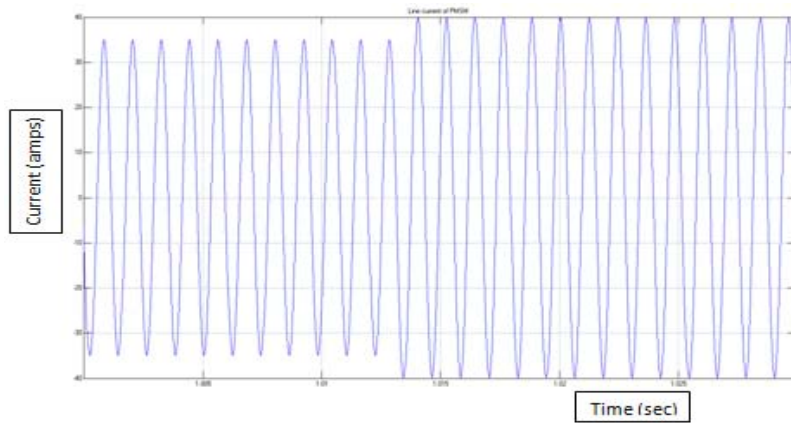


**Figure 16:** Speed Variation of PMSM

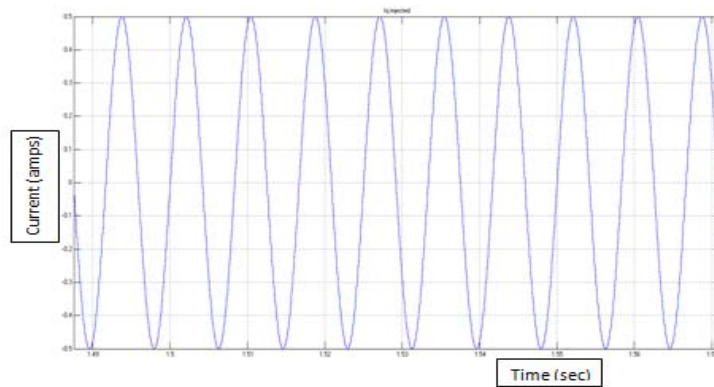


**Figure 17:** Active power variation during motoring/generating mode at the grid side of MTG

Fig 18 shows the Line Current of the PMSM operating in both Motoring mode and Generating mode. At the time of switching from Grid connected to Islanding operation at 1 sec, there is increase in line current of PMSM. Fig. 19 shows the reactive component of current injected into the grid for zero reference value of  $i_q$ .

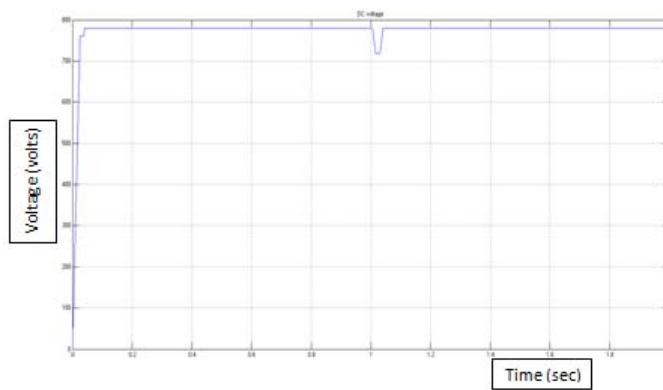


**Figure 18:** Line current of PMSM



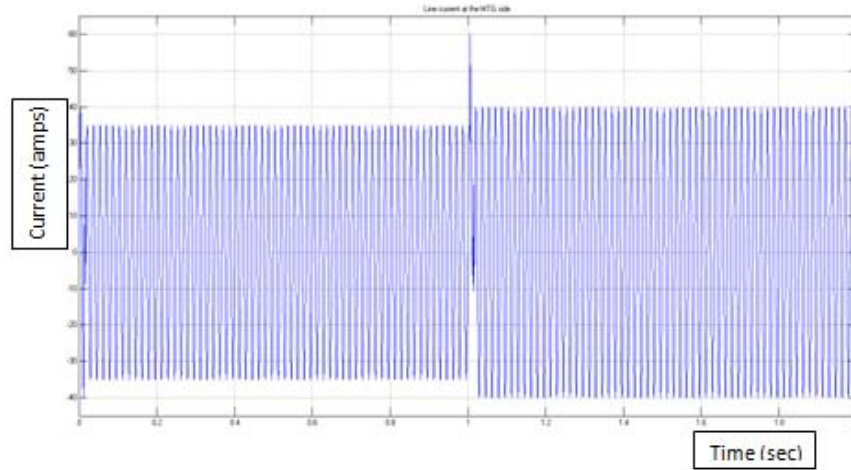
**Figure 19:** Injected current  $i_q$  into the grid

Fig. 20 shows the DC bus voltage regulated at 760 V when the machine is operating in grid-connected mode. At the time of switching from Grid connected to Islanding operation there is dip in DC link voltage as shown in the figure.



**Figure 20:** DC Link voltage

At  $t=1$  sec, the interface circuit breaker between MTG system and grid is opened and the voltage-frequency (Vf) control scheme for island operation is activated. Fig. 21 shows the line current variation of MTG system both during grid connected and islanding operations.



**Figure 21:** Line current at the MTG side

The terminal voltage at the load is shown in Fig. 22 when MTG system is operating at both Grid connected and Islanding mode

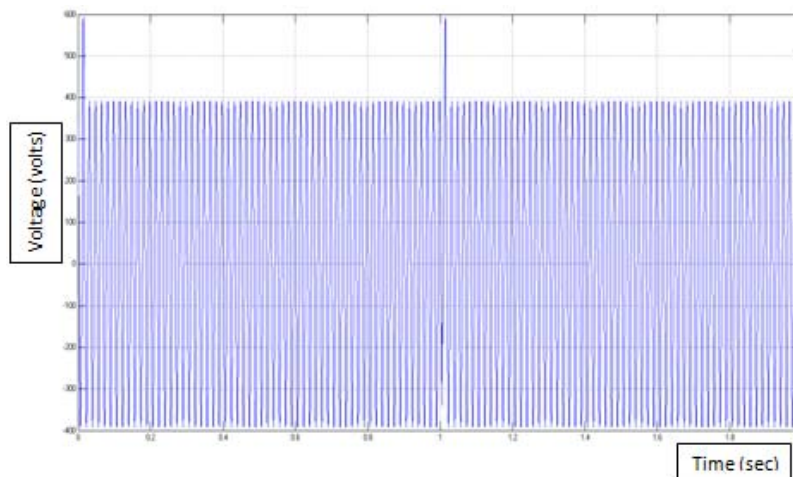


**Figure 22:** Voltage across the load terminal

Fig. 23 shows that the Load Current remains constant both during the Grid connected and Islanding mode.

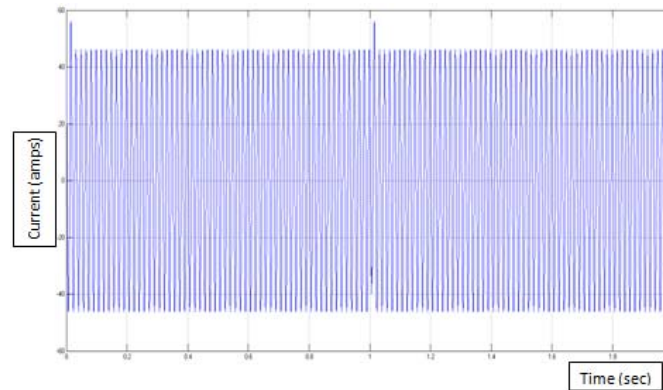


**Figure 23:** Line current variation of the load

## Conclusions

The detailed dynamic model of each of the system component has been developed and the system models are implemented under SIMULINK environment. The micro turbine operation during initial motoring and thereafter generating mode has been studied. The performance during grid connection and islanding has also been studied. The following conclusions are drawn from this study:

Very small duration transients are observed when the micro turbine operation is changed from grid mode to islanding mode. Further, during islanding, the line current of permanent magnet synchronous machine is high.

The microturbine initially operates in motoring mode before attaining the generating mode operation.

## Appendix Simulation parameters for the MTG system

Grid parameters	480V, 60Hz, $R_s = 0.4\Omega$ and $L_s = 2\text{Mh}$
Filter parameters	$L = 0.97\text{mH}$ , $R = 0.21\Omega$
Switching Frequency	Grid side converter = 8Khz Machine side converter = 20Khz
DC link capacitance	500 $\mu\text{F}$
PI controllers sampling time	100 $\mu\text{sec}$
PMSM parameters	480V, 30kW, 1.6Khz, 96000rpm, $R_s = 0.25\Omega$ , $L_q = L_d = 0.0006875\text{H}$
Microturbine parameters	Gain (K) = 25, X = 0.4, Y = 0.05 and Z = 1

## References

- [1] Amer Al-Hinai and Ali Feliachi, "Dynamic model of a microturbine used as a distributed generator" System Theory 2002, Proceedings of the 34<sup>th</sup>

- Southeastern Symposium on, Huntsville, Alabama, 18-19 March 2002, pp. 209-213.
- [2] W. G. Scott, "Micro-Turbine Generators for Distribution Systems," IEEE Applications Magazine, Vol. 4, Issue 4, pp. 57-62, May/June, 1998.
  - [3] W. I. Rowen, "Simplified mathematical representations of heavy duty gas turbines," Journal of Engineering for Power, Transactions ASME, vol. 105, no. 4, pp. 865-869, Oct, 1983.
  - [4] L. N. Hannet and Afzal Khan, "Combustion turbine dynamic model validation from tests," IEEE Transactions on Power Systems, vol. 8, no. 1, pp. 152-158, Feb. 1993.
  - [5] A. Cano, F. Jurado and J. Carpio, "Influence of micro-turbines on distribution networks stability," in Proceedings, IEEE PES General Meeting, vol. 4, pp. 2153-2158, Jul. 2003, Toronto, Canada.
  - [6] Amer Al-Hinai and Ali Feliachi, "Dynamic model of a microturbine used as a distributed generator," in Proceedings, 34th Southeastern Symposium on System Theory, Huntsville, pp.209-213, Alabama, March 2002.
  - [7] Bimal K. Bose, Modern Power Electronics and AC Drives, Pearson Education, 2003.
  - [8] D. N. Gaonkar and R. N. Patel, "Modeling And Simulation Of Microturbine Based Distributed Generation System", Proceedings of IEEE Power India Conference, New Delhi, pp. 5, April, 2006
  - [9] N. Mohan, T. M. Undeland, and W. P. Robbins, "Power Electronics, Converters, Applications and Design," 2nd Edition, John Wiley & Sons.
  - [10] Gaonkar, D. N., Pillai, G. N., and Patel, R. N., (2008), Dynamic performance of microturbine generation system connected to grid, *Journal of Elect. Power Compon. Syst.*, Vol. 36, No. 10, pp. 1031–1047, 2008.
  - [11] Chung, S.-K., (2000), Phase-locked loop for grid-connected three-phase power conversion systems, *Proc. Inst. Elect. Eng.*, Vol. 147, No. 3, pp. 213–219, 2000.